CONF-960738--9
SAND--96-8559C

IMPROVING CONVERGENCE RATES FOR LOW PRESSURE MATERIAL PROCESSING CALCULATIONS

Christopher D. Moen *
Sandia National Laboratories
Livermore, CA 94551-0969

RECEIVED
NOV 0 6 1996
OSTI

ABSTRACT

An enhanced solution strategy for the SIMPLER algorithm is presented for low pressure heat and mass transport calculations with applications in material processing. The accurate solution of highly diffusive flows requires an inflow boundary condition that preserves chemical species mass fluxes. The flux-preserving inflow boundary condition contains a scaling problem that causes the species equations to converge very slowly when using the standard SIMPLER algorithm. A gradient algorithm, coupled to a line-relaxation method, accelerates the convergence of the linear problem. Reformulation of the pressure-correction boundary conditions ensures that continuity is preserved in each finite volume at each iteration. The boundary condition scaling problem is demonstrated with a simple linear model problem. The enhanced solution strategy is implemented in a baseline computer code that is used to solve the multicomponent Navier-Stokes equations on a generalized, multiple-block grid system. Convergence rate acceleration factors of up to 100 are demonstrated for several material processing example problems.

NOMENCLATURE

A	=	boundary area
D	=	average Fickian mass diffusivity
j	=	mass diffusion flux
$\dot{m}$	=	mass flow rate
$\mathbf{n}$	=	unit normal vector to boundary
Pe	=	Peclet number
u	=	velocity
x	=	Cartesian coordinate
Y	=	mass fraction
$\overline{Y}$	=	reference mass fraction
Δ	=	finite-difference increment
∇	=	gradient operator
ϕ	=	potential function
ρ	=	density

Subscripts

g	=	chemical species
1	=	ghost-cell point
2	=	first interior point

*Senior Technical Staff, Thermal and Plasma Processes Department, (510) 294-3709

INTRODUCTION

Numerical simulation is a useful tool for studying heat and mass transfer in gas-phase manufacturing of materials. Numerical models predict the uniformity and deposition rate of material coatings and help design reactors and processes. Many applications occur at low pressures, such as etching and chemical vapor deposition, (Jensen, *et al.*, 1991) and (Kleijn, 1991a). Segregated solutions algorithms are commonly used for chemical vapor deposition (CVD) modeling, (Evans and Greif, 1994), (Kleijn, *et al.*,1889), and (Kleijn and Hoogendoorn, 1991b). Though they can be slow, they are desirable for their simplicity and economic use of computer resources. Increased coupling between equations improves convergence for some flow regimes, discussed in the review by Patankar (1988). Fully coupled methods, (Jensen, 1991) and (Knoll, *et al.*, 1995), are used for reacting flow, but at the cost of storing large matrices. For many applications, the coupled species transport equations are split from the heat and momentum equations (Moffat and Jensen, 1986,1988).

For highly diffusive problems, equation coupling is not as important as spatial coupling. Convergence is degraded at low pressures by poor numerical propagation of information between physical boundaries. Mass diffusivities increase with decreasing pressure and gradients in species composition can span an entire reactor. Difficulty arises at the inflow boundary where convection must balance diffusion to preserve specified species mass fluxes. Information propagates very slowly from such a boundary for a particular class of segregated solution algorithms with explicit updating of boundary conditions. Boundary condition equations should be coupled to interior equations with complete solution of the resulting lineared system.

The focus of this paper is to explain the physical processes that adversely affect the convergence rate at low pressures and modify the solution algorithm accordingly. The algorithm enhancements discussed in this article may not be beneficial to fully coupled schemes. Solution algorithm enhancements are demonstrated with a baseline computational fluid dynamics (CFD) code based on the SIMPLER algorithm (Patankar, 1980). The baseline code, CURRENT, is an extensive reformulation of the TEACH (Gosman and Pun, 1973) code by Evans (1994). He recast the governing equations in terms of a generalized body-fitted coordinate system with multiple-block grids

DISTRIBUTION OF THIS DOCUMENT IS UNLIMITED

MASTER

DISCLAIMER

Portions of this document may be illegible in electronic image products. Images are produced from the best available original document.

DISCLAIMER

This report was prepared as an account of work sponsored by an agency of the United States Government. Neither the United States Government nor any agency thereof, nor any of their employees, makes any warranty, express or implied, or assumes any legal liability or responsibility for the accuracy, completeness, or usefulness of any information, apparatus, product, or process disclosed, or represents that its use would not infringe privately owned rights. Reference herein to any specific commercial product, process, or service by trade name, trademark, manufacturer, or otherwise does not necessarily constitute or imply its endorsement, recommendation, or favoring by the United States Government or any agency thereof. The views and opinions of authors expressed herein do not necessarily state or reflect those of the United States Government or any agency thereof.

and implemented multicomponent transport with gas-phase and surface-phase chemical reactions. Strengthening the implicit coupling between physical boundaries and across internal grid-block boundaries in the baseline code greatly enhances convergence. Furthermore, convergence rates are improved with only modifications to the species and continuity algorithms.

The solution algorithm enhancements affect both the nonlinear and linear parts of the SIMPLER algorithm. The nonlinear part is modified by including the boundary condition equations in the linearization of the transport equations. Coupling the boundary conditions allows the boundaries to directly communicate at each iteration, but it is during the solution of the linear problem in which information is numerically propagated. The convergence of the linear problem is accelerated by adding the generalized minimal residual (GMRES) gradient scheme of Saad and Schultz (1986) to the line-relaxation scheme. The gradient algorithm is matrix-free, described by Wigton *et al.* (1985) and is implemented with only minor modifications to the existing code. The solution of the continuity equation must also be modified to keep up with the improved species algorithm.

The following sections discuss the baseline code and the developments which lead to the enhanced solution strategy. First, the solution of the governing equations with the baseline solution algorithm is discussed. Then, the low pressure convergence problems are investigated for a simple model problem. Lessons from the model problem lead to modifications to the baseline solution algorithm and boundary condition treatment. Improved performance is demonstrated for two example chemical reactor problems.

TRANSPORT EQUATIONS

The governing equations used in this work, (Evans and Greif, 1994) and (Kleijn,1989), describe the conservation of mass and the transport of momentum, energy, and chemical species, and are suitable for chemically reacting flows with multicomponent transport. The low Mach number approximation is used where the pressure is split into dynamic and thermodynamic parts and the viscous dissipation term is dropped from the thermal energy equation.

There are two types of boundary conditions: conditions at physical boundaries and conditions at grid-block interfaces. The interface conditions are the result of the block-by-block solution algorithm for the linearized equations. Ghost-cells are used around the grid-blocks to calculate fluxes and averages at boundaries and interfaces. Most boundary conditions are updated explicitly in the baseline CFD code. The ghost-cells, used to couple grid blocks along block interfaces, are locally explicit, but are updated during line-relaxation sweeps so that information propagates across the blocks.

Dirichlet conditions are traditionally applied at an inflow boundary, but they may not preserve the correct species mass flow rates when the flow is highly diffusive. If there is a gradient in chemical composition near the inflow boundary, then the more stringent condition for preserving species mass fluxes is applied:

$$\frac{\dot{m}_g}{A} = \rho u Y_g + \mathrm{j}_g. \tag{1}$$

which states that the species mass flux is balanced by the convective flux and the diffusive flux. The correct composition of chemical species entering the reactor is artificially imposed instead of moving the grid boundaries far away from the source of the composition gradient.

At an outflow boundary, variables are extrapolated from the interior to the ghost-cells. The boundary velocity is also extrapolated from the interior. Since the extrapolation for the boundary velocity does not necessarily satisfy continuity, the outflow velocities are scaled to satisfy global mass conservation.

LOW PRESSURE CONVERGENCE PROBLEM

The root of the low-pressure convergence problem is the unfavorable scaling within the chemical species mass flux-preserving inflow boundary condition, applied in highly diffusive regions. A simple linear model problem is used to demonstrate how convergence degrades with the species cell-Peclet number.

Chemical reaction rates, which usually cause convergence problems in reacting flow computations, play a lesser role in the convergence rate degradation. The reactions are relatively slow at low pressure and not very energetic so there is not a strong effect on the temperature. Surface chemistry is more problematic than gas-phase chemistry since it provides highly nonlinear sources and sinks for gas-phase species at physical boundaries.

Peclet Number Scaling

A scaling problem between convection and diffusion is artificially introduced by using a flux-inflow-boundary condition near a strong species composition gradient. For low Peclet numbers, diffusive transport dominates convective transport. Yet, for the limiting case of uniform inflow composition and no chemical reactions, the convective transport term determines the species distribution within the flow domain. The Peclet number scaling makes it difficult to enforce the convective part of the boundary condition. The scaling is demonstrated using the inflow boundary condition, Eq. (1), simplified by the assumption of Fickian diffusion:

$$\frac{\dot{m}_g}{A} = \rho u Y_g - \rho D \frac{\partial Y_g}{\partial x}. \tag{2}$$

Dividing by the total mass flux gives:

$$\overline{Y}_g = Y_g - \frac{D}{u}\frac{\partial Y_g}{\partial x}, \tag{3}$$

where $\overline{Y}_g = \dot{m}_g/\dot{m}$ represents the reference inflow mass fraction for species g. The cell-Peclet number, $\mathrm{Pe}_{\Delta x}$, is defined by the length scale of the finite volume, Δx, the convective velocity, and a mass diffusivity, D: $\mathrm{Pe}_{\Delta x} = u\Delta x/D$. The boundary condition is discretized about the

inflow cell face using centered differences and the explicit formula for updating the boundary point is:

$$Y_{g,1} = \frac{1 - \frac{1}{2}\mathrm{Pe}_{\Delta x}}{1 + \frac{1}{2}\mathrm{Pe}_{\Delta x}} Y_{g,2} + \frac{\mathrm{Pe}_{\Delta x}}{1 + \frac{1}{2}\mathrm{Pe}_{\Delta x}} \overline{Y}_g. \tag{4}$$

For small limiting values of the cell-Peclet number, the ghost-cell mass fraction is more dependent on the interior point, $Y_{g,2}$ than the reference value, $\overline{Y}_g$, during the explicit update. Yet, the mass fractions must approach the reference value when there are no chemical reactions or sources.

$$\lim_{\mathrm{Pe}_{\Delta x} << 1} Y_{g,1} = Y_{g,2} + \mathrm{Pe}_{\Delta x} \overline{Y}_g \tag{5}$$

Bad initial guesses for the mass fractions result in very slow convergence to the actual solution. The interior points are strongly dependent on the boundary points because of the elliptic nature of the partial differential equations. The scaling argument indicates that any implicit scheme used to update interior points without coupling the boundary points is ineffective.

Linear Model Problem

The severity of the Peclet number scaling problem is demonstrated using a simple linear model problem. The model approximates the multicomponent transport processes with simple diffusion, described by the Laplace equation:

$$\nabla^2 \phi = 0. \tag{6}$$

The "mass flux preserving" inflow boundary condition is set over part of the boundary and the rest of the boundary has a zero-gradient condition:

$$\phi - \frac{1}{\epsilon} \nabla\phi \cdot \mathbf{n} = 1, \tag{7}$$

$$\nabla\phi \cdot \mathbf{n} = 0, \tag{8}$$

where $\mathbf{n}$ is the unit normal vector to the boundary. The Peclet number scaling is introduced as the parameter, ϵ, even though there is no convection in the model. The solution to these equations is $\phi = 1$ and the initial condition is $\phi = 0$. For the purposes of discussion, the scaling parameter ϵ will be referred to as the Peclet number, Pe.

Equations (6) through (8) are discretized using centered differences on a uniform multiple-block grid. The scalar variable, ϕ, is located at the center of volumes formed by grid points. The mesh consists of three grid blocks, each of size 31×11 points. The blocks stack on top of each other to form a square grid, shown in Fig. 1, with cells of unit length. The "inflow boundary" is the west face of the bottom Block 1. The discrete linear equations are solved using a line-relaxation scheme, each iteration consisting of four sweeps in alternating directions.

A large number of line-relaxation iterations are required to solve the equations when the scaling is poor (small Peclet number) and the boundary conditions are evaluated explicitly. The convergence is plotted as a function of the L_2-norm of the linear system residual in Fig. 2. The number of iterations required to converge the problem scales with $(\frac{1}{2} + \frac{1}{\mathrm{Pe}})$. As the Peclet number increases, the number of iterations required to converge the problem with the flux inflow boundary condition approaches that for a fixed Dirichlet boundary condition, $\phi = 1$.

Implicit coupling of the physical boundary conditions in the line-relaxation scheme improves convergence by 25%, but the work required is still excessive. The boundary information is propagated implicitly in the direction of the line-solve, but more "explicit-like" in the sweep direction. The full set of boundaries, which drive the interior equations, are not directly coupled. Each boundary point should simultaneously see every other boundary point.

Matrix-free, preconditioned gradient algorithms provide an efficient solution to the boundary communication problem. The method is similar to direct inversion, but there is no need to store inverse-matrix fill-in. The GMRES gradient algorithm is used to invert the linear system with the block-by-block line-relaxation implicit scheme acting as a preconditioner. The GMRES scheme enhances the implicitness of the line-relaxation scheme. The gradient algorithm is not restarted for the model problem and the number of search directions is limited to 20 so that outer iterations on the problem are required. The convergence history for the enhanced implicit scheme is shown in Fig. 3. The residual norm is plotted as a function of the number of preconditioning calls. Each preconditioning call is comparable in computational work to one iteration of the line-relaxation scheme alone. The overhead work of the gradient algorithm effectively increases the amount of CPU time required for each preconditioner call by 30%. The addition of the GMRES scheme accelerates the convergence of the line-relaxation scheme by anywhere from a factor of 4 to 1000, depending on the cell-Peclet number.

The GMRES acceleration scheme provides no additional benefits as the mesh density is refined. The amount of work required to converge on a finer mesh follows theoretical scaling laws for relaxation-type schemes. When the number of mesh points is increased by a factor of 16 to three 121×41 grids, the number of iterations required to reach the convergence tolerance increases by roughly an order of magnitude. The convergence rate for the GMRES accelerated scheme on the denser grid behaves similarly to the line-relaxation itself, shown in Fig. 4.

ENHANCED NAVIER-STOKES ALGORITHM

The solution algorithm enhancements to the Navier-Stokes code involve the species equations and the pressure-correction equation. The modifications to the species equations follow those described for the model problem where the boundary condition equations are treated implicitly and the linear problem is solved to completion with the GMRES algorithm. When the linearized species equations are fully converged, the solution can change too fast for the nonlinear problem and the overall solution strategy becomes unstable. Stability is increased by satisfying the continuity equation more rigorously.

Errors in continuity cause artificial sources and sinks in the species equations. In the baseline algorithm, neither continuity nor the linearized species equations are satisfied exactly at each iteration. The errors tend to offset each other and no stability problems result. Conversely, the enhanced solution algorithm does such a good job of satisfying the transport equations that they become very sensitive to mass errors.

The solution to the continuity problem is twofold. First, it is recognized that continuity errors during iteration are due to the use of zero-gradient boundary conditions for the pressure-correction on all boundaries and incomplete convergence of the linear pressure-correction equation. The zero-gradient boundary condition on the pressure-correction term does not allow outflow boundary velocities to change. The outflow boundary condition is reformulated so that the outflow velocity can be corrected in a manner consistent with continuity. Secondly, the matrix-free GMRES gradient algorithm is added to the solution algorithm for the pressure-correction equation to accelerate convergence.

The pressure-correction procedure is reformulated in a manner consistent with other projection methods for low Mach number flows, (Chorin, 1967) and (Dwyer, 1994). The pressure is still updated according to the SIMPLER algorithm. The pressure-correction is treated as a velocity potential and is set to zero at the outflow boundary ghost points. Matrix coefficients are extrapolated from the interior. A velocity correction can then be formulated at the outflow boundary and the velocity updated in a way that is consistent with continuity. The velocity potential approaches the fixed boundary value of zero everywhere upon overall convergence.

EXAMPLE PROBLEMS

Two manufacturing process examples are presented to demonstrate the convergence performance of the enhanced solution strategy. All example problems are run on a Hewlett Packard 735/125 workstation. The baseline code is compiled for 32-bit precision floating-point arithmetic and the modified code is compiled for 64-bit precision. The modified code must be compiled at 64-bit precision in order to avoid numerical precision problems with the gradient algorithm. The discrete governing equations in the code are solved using dimensional quantities in terms of the metric cgs system.

SiO_2 Deposition

Silicon dioxide dielectric growth in a rotating disk chemical vapor deposition (CVD) reactor is modeled. This problem involves gas-phase and surface-phase chemistry in a diffusive environment. The baseline CFD code does not exhibit extremely poor convergence rates for this problem, but the enhanced code improves the average convergence time by a factor of two.

In the CVD reactor, a tetraethoxysilane (TEOS) precursor gas is injected through a shower head arrangement onto a heated substrate, supplying the silicon and oxygen for the deposition. The heat applied to the substrate conducts into the flow field and dissociates the TEOS into other chemical precursors. The chemical precursors react at the substrate with intermediate surface species to form silicon dioxide.

The reactor geometry is discretized with finite volumes in a body-fitted coordinate system. The reactor grid, shown in Fig. 5, is constructed from three blocks with the following block sizes: 21×41, 21×16, and 21×16 grid points. Radial position is measured relative to the vertical centerline and axial position is measured relative to the base of the outflow face. Only half the grid is used for the computation since the reactor is axisymmetric about the vertical centerline. The thermodynamic pressure in the reactor is 1 torr. The growth substrate is maintained at 1000 K and rotates at 30 rpm. The process gas, a mixture of nitrogen and TEOS shown in Table 1, flows into the reactor at 300 K. The axial temperature distribution along the outer vertical wall is represented by a piecewise linear curve, given in Table 2.

Table 1: TEOS Inflow Conditions as a Function of Radial Position

	Inner 5.08 cm	Outer 5.08 cm
X_{TEOS}	0.5	0.75
X_{N_2}	0.5	0.25
V_{in}	20 cm/s	30 cm/s

Table 2: Wall Temperature Profile as a Function of Axial Position

Axial Position (cm)	Temperature (K)
0.0	300.0
2.54	320.0
5.08	400.0
7.62	380.0
10.16	340.0

The gas-phase species considered in the model are: N_2, $Si(OC_2H_5)_4$, $Si(OH)(OC_2H_5)_3$, C_2H_5OH, C_2H_4, and H_2O. A single gas-phase reaction describes the thermal decomposition of TEOS into triethoxysilanol and ethene:

$$Si(OC_2H_5)_4 \rightleftharpoons Si(OH)(OC_2H_5)_3 + C_2H_4.$$

The water and ethanol species are byproducts of the surface-phase reaction mechanism, given in Table 3. A short-hand notation is used involving the symbol G for describing the intermediary glass-like surface species required to form bulk dielectric, $SiO_2(D)$. The notation (D) indicates the solid material in this mechanism. The computational solution indicates that the chemical precursors are fairly well distributed across the substrate surface. One of the primary chemical radical precursors to the silicon dioxide deposition is $Si(OH)(OC_2H_5)_3$, shown in Fig. 6.

Table 3: TEOS Surface-Phase Reaction Mechanism

	Reaction
1.	$Si(OC_2H_5)_4 + SiG3(OH) \rightleftharpoons SiO_2(D) + SiGE3 + C_2H_5OH$
2.	$SiG3E \rightleftharpoons SiG3(OH) + C_2H_4$
3.	$SiG(OH)E2 \rightleftharpoons SiG(OH)2E + C_2H_4$
4.	$SiGE3 \rightleftharpoons SiG(OH)E2 + C_2H_4$
5.	$SiG(OH)2E \rightleftharpoons SiG3(OH) + C_2H_5OH$
6.	$SiG(OH)E2 \rightleftharpoons SiG3E + C_2H_5OH$
7.	$SiG(OH)2E \rightleftharpoons SiG3E + H_2O$
8.	$Si(OH)(OC_2H_5)_3 + SiG3(OH) \rightleftharpoons SiO_2(D) + SiGE3 + H_2O$

The cell-Peclet numbers at the inflow boundary are close to values that begin to cause convergence problems for the model problem. The species Peclet numbers are based on the inflow conditions and are given for a unit reference length of one centimeter: $Pe_{N_2} = 0.27$ to 0.57 and $Pe_{TEOS} = 2.0$ to 4.2. These numbers are multiplied by the wall-normal grid spacing of 0.35 cm to form the cell-Peclet numbers.

Solutions generated with the baseline code and the modified code use mostly the same input parameters. The baseline code uses an under-relaxation value of 0.5 for the temperature equation and 0.9 for the species equations. With the modified solver, the species equations are damped at a value of 0.5 and the temperature equation is damped at a value of 0.9.

The convergence rate for this problem, shown in Fig. 7, is measured in terms of the L_1-norm of the species equation. The L_1-norm is constructed from flux balances over each control volume for each species equation, scaled by the maximum species convective flux. Only the residual norm for the species equations is plotted since it is most indicative of convergence problems. The baseline code converges to the level of 10^{-6} after 4000 iterations at which point it reaches the limits of numerical precision. The baseline code runs at a rate of 0.8 seconds per iteration (averaged over 7500 iterations). The modified code with the gradient algorithm runs at a rate of 2.5 seconds per iteration (averaged over 1000 iterations). One iteration of the modified code requires many calls to the line-relaxation preconditioner. The iteration rate for the modified code varies slightly due to the variable search direction strategy in the gradient scheme.

There are actually two measures of convergence. The mathematical residual norm describes how well the discrete governing equations have been satisfied. If this measure is used, the modified code converges to the L_1-norm of 10^{-6} twenty times faster than the baseline code. At this same convergence level, the baseline code is converged as far as numerical precision will allow. The residual norm can be misleading since physical quantities of interest often converge to within engineering accuracy long before the residual norm reaches the limits of computer precision. The second measure of convergence is based on the physical quantities that are to be extracted from the simulation. The number of iterations required to converge to engineering accuracy is found by studying surface heat and mass flux profiles at the substrate. Even though the modified code runs about three times slower per iteration than the baseline code, the modified code converges to an engineering solution twice as fast as the baseline code.

Methyltrichlorosilane Injection

The injection and mixing of cold methyltrichlorosilane (MTS) gas, CH_3SiCl_3, into hot helium gas is modeled for a silicon carbide CVD flow-tube experiment. A mixing chamber is designed such that the gases mix completely and flow uniformly out the exhaust.

The geometry consists of a cylindrical center plug with normal injectors inside a cylindrical mixing chamber, shown in Fig. 8. The center plug, with a spherical cap, is 2.5 cm in diameter and the mixing chamber is 5.0 cm in diameter. The injectors are 1.0 mm in diameter and are modeled as a continuous ring. The grid system consists of five blocks of size: 26×26, 7×26, 11×26, 36×21, and 36×26 grid points. Only half the grid is used for the computations since it is symmetric about the axial centerline.

The flow-tube model is not a low pressure problem, but it is very diffusive. The thermodynamic pressure is 100 torr. The MTS flows in at a rate of 500 sccm and a temperature of 300 K. The helium flows in at a rate of 4500 sccm and a temperature of 1400 K. The mole fraction of MTS for complete mixing is 0.1.

The cell-Peclet number at the helium inflow is low enough that convergence problems are expected. The species Peclet numbers are based on the inflow conditions and are given for a unit reference length: $Pe_{He} = 0.037$ and $Pe_{MTS} = 300.0$. These numbers should be multiplied by the wall-normal grid spacing of 0.367 cm for helium and 0.0346 cm for MTS to find the cell-Peclet numbers.

In addition to boundary condition scaling problems in the linear problem, there are transport property problems which affect the stability of the nonlinear iteration process. The mixing configuration is hard to solve because the injected gas has a molecular weight of 149.5 and the carrier gas has a molecular weight of 4. The MTS mass fraction in the completely mixed gas is about 0.8 even though the volume fraction is low. The disparities in molecular weight and transport properties cause numerical problems during the iterative phase of the nonlinear solution procedure. When the solution procedure is started, the MTS injection is impulsive. If the linearized species equations are solved exactly at each nonlinear iteration, large nonphysical errors are introduced. Solution damping is ineffective for this problem. The error is controlled by limiting the degree to which the linear problem is converged. The number of search directions for the gradient solver is selected such that the boundary conditions boundary conditions remain coupled, but not so many that physical errors from the incorrect transport properties dominate. Even with strict limits on search directions, the strong coupling between boundaries is maintained.

The convergence history for the species equations, in terms of the scaled L_1-norm of the conservation laws, is plotted in Fig. 9. The converged mixing levels are

approached after about 200 iterations. The modified code runs at about six seconds per iteration for this problem. The convergence history for the baseline code is not shown because it is prohibitively slow for this case. Well over 100000 iterations are required with the baseline code. The modified code provides an acceleration of at least a factor of 100 over the baseline code.

SUMMARY

An enhanced solution strategy for the SIMPLER algorithm is presented for low pressure heat and mass transport calculations with applications in material processing. The solution strategy is implemented in an existing baseline computer code that is used to solve the multicomponent Navier-Stokes equations on a generalized, multiple-block grid system.

The adverse interaction between the inflow boundary condition scaling and the implicit line-relaxation scheme is demonstrated using a simple linear model problem. The convergence rate degrades with the species cell-Peclet number. The physical boundaries do not communicate directly during relaxation sweeps. Enhancing the solution algorithm for the linear problem with a gradient algorithm increases the convergence rate by at least two orders of magnitude. The preconditioned gradient algorithm accelerates the convergence, but the convergence rate is still proportional to the grid size. Future considerations should include the use of multigrid methods for mesh independent convergence rates.

The solution strategy modifications are consistent with the segregated solution approach of the SIMPLER algorithm. Segregation is much more attractive than using a fully coupled Newton method because it is easier to increase the chemical complexity without running out of computing resources. The code modifications are relatively nonintrusive, requiring few changes to validated sections of code. The boundary condition equations are coupled to the interior equations for the linearization. The linear problem is solved completely at each nonlinear iteration using a gradient method to accelerate the existing line-relaxation method. The modifications are only applied to the species equations and the pressure-correction equation. Boundary conditions for the pressure-correction equation are reformulated to ensure continuity is preserved in each finite volume at each iteration.

REFERENCES

Chorin, A. J., 1968, "Numerical Solution of the Navier-Stokes Equations". *Mathematics of Computation*, **22**(1):745–762.

Dwyer, H., 1991, "Calculation of Low Mach Number Reacting Flows". *AIAA Journal*, **28**(1):98–105.

Evans, G. and R. Greif, 1994, "A Two-Dimensional Model of the Chemical Vapor Deposition of Silicon Nitride in a Low-Pressure Hot-Wall Reactor Including Multicomponent Diffusion". *International Journal of Heat and Mass Transfer*, **37**(10):1535–1543.

Gosman, A. D. and W. M. Pun, 1973, "Calculation of Recirculating Flow". Unpublished lecture notes, Imperial College of Science and Technology.

Jensen, K. F., D. I. Fotiadis, and T. J. Mountziaris, 1991, "Detailed Model of the MOVPE Process". *Journal of Crystal Growth*, **107**:1–11.

Kleijn, C. R., Th. H. van der Meer, and C. J. Hoogendoorn, 1989, "A Mathematical Model for LPCVD in a Single Wafer Reactor". *Journal of the Electrochemical Society*, **136**(11):3423–4333.

Kleijn, C. R., 1991a, "On the Modelling of Transport Phenomena in Chemical Vapour Deposition and Its Use in Reactor Design and Process Optimization". *Thin Solid Films*, **206**:47–53, December 1991.

Kleijn, C. R. and C. J. Hoogendoorn, 1991b, "A Study of 2- and 3-D Transport Phenomena in Horizontal Chemical Vapour Deposition Reactors". *Chemical Engineering Science*, **46**(1):321–334.

Knoll, D. A., P. McHugh, and D. Keyes, 1995, "Newton-Krylov Methods for Low Mach Number Combustion". In 12^{th} *Computational Fluid Dynamics Conference*, AIAA Paper 95–1672.

Moffat, H. and K. F. Jensen, 1986, "Complex Flow Phenomena in MOCVD Reactors: I. Horizontal Reactors". *Journal of Crystal Growth*, **77**:108–119.

Moffat, H. and K. F. Jensen, 1988, "Three-Dimensional Flow Effects in Silicon CVD in Horizontal Reactors". *Journal of the Electrochemical Society*, **135**(2):459–471.

Patankar, S. V., 1980, *Numerical Heat Transfer and Fluid Flow*. Hemisphere Publishing Company.

Patankar, S. V., 1988, "Recent Developments in Computational Heat Transfer". *Journal of Heat Transfer*, **110**:1037–1045.

Saad, Y. and M. H. Schultz, 1986, "GMRES: A Generalized Minimal Residual Algorithm for Solving Non-symmetrical Linear Systems". *SIAM Journal of Scientific and Statistical Computing*, **7**(3):856–869.

Wigton, L. B., N. J. Yu, and D. P. Young, 1985, "GMRES Acceleration of Computational Fluid Dynamics Codes". AIAA Paper 85–1494, 7^{th} Computational Fluid Dynamics Conference.

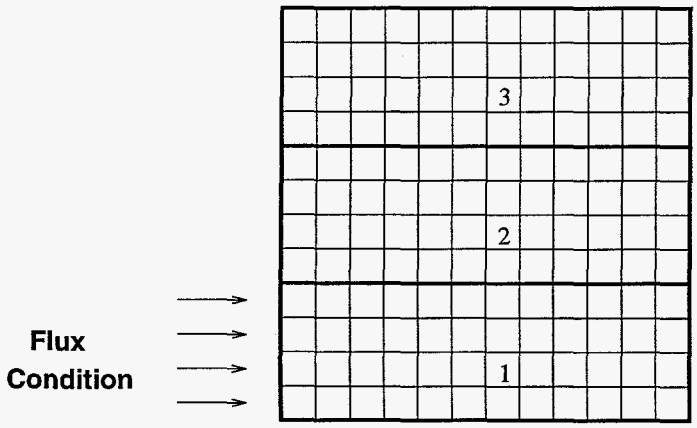

Figure 1: Three-Block Grid for Model Problem

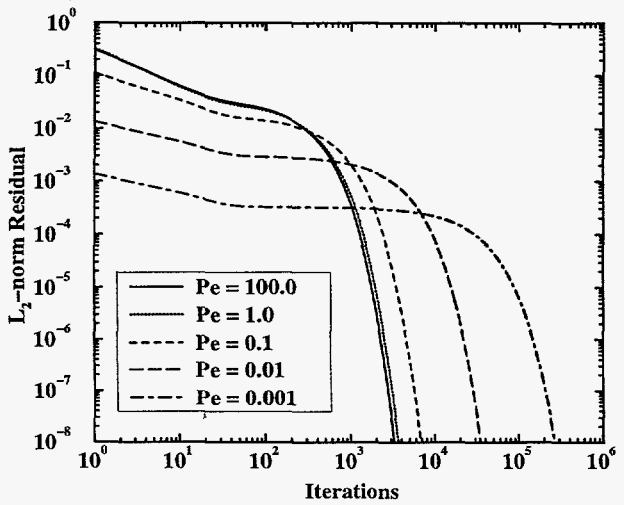

Figure 2: Line-Relaxation Convergence Scales Inversely with Peclet Number

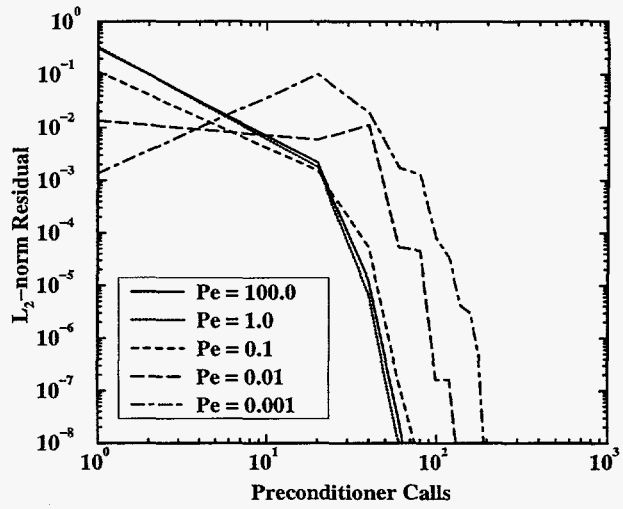

Figure 3: Line-Relaxation Convergence is Accelerated by GMRES

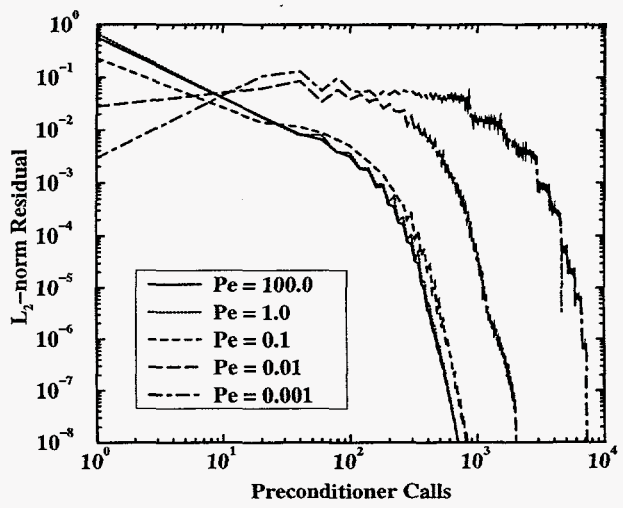

Figure 4: Line-Relaxation Convergence Accelerated by GMRES on Denser Grid

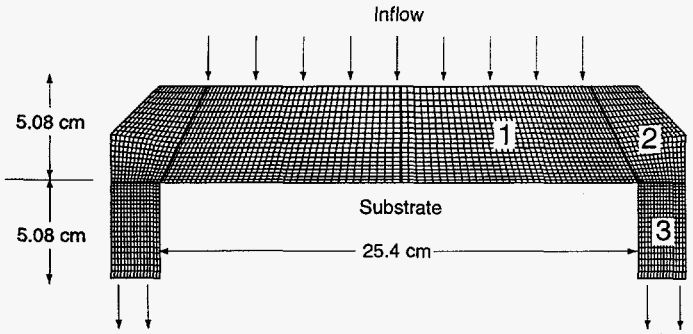

Figure 5: Three-Block Grid for TEOS Reactor

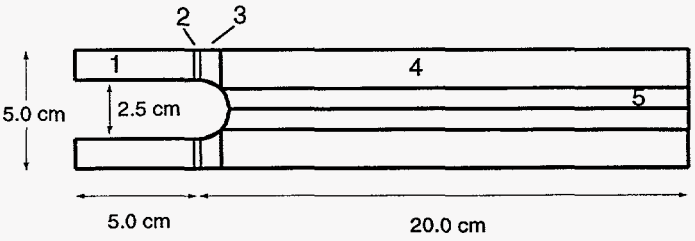

Figure 8: Five-Block MTS Grid System

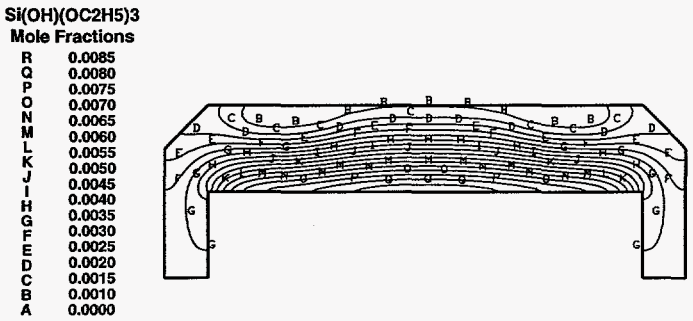

Figure 6: Triethoxysilanol Mole Fraction Contours in TEOS Reactor

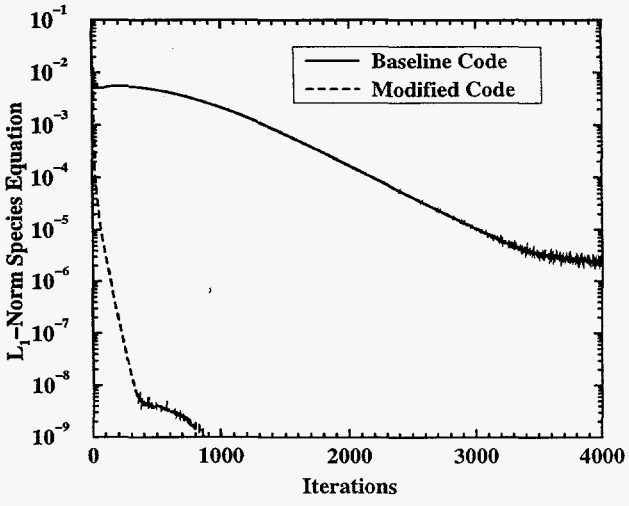

Figure 7: Convergence History for TEOS Problem

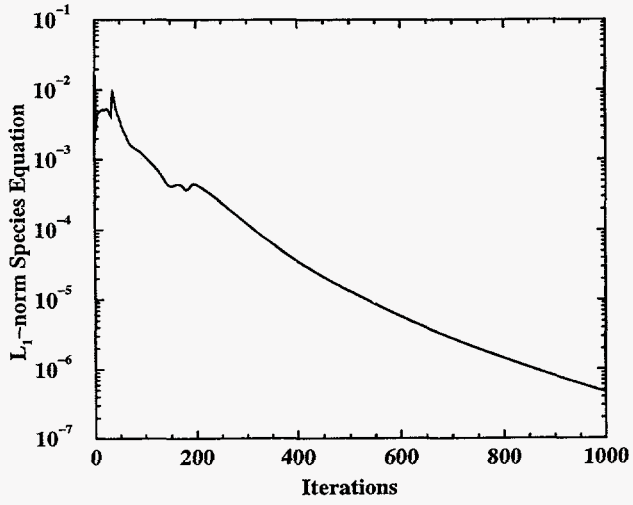

Figure 9: MTS Convergence Performance for Enhanced Solution Strategy